

# Influence of physical interactions on the porosity of gelatin-alginate scaffolds

D. M. DRAGUSIN, D. E. GIOL, E. VASILE<sup>a</sup>, R. TRUSCA<sup>a</sup>, M. TEODORESCU, I. STANCU, D. S. VASILESCU<sup>\*</sup>, H. IOVU

*University Politehnica of Bucharest, 149 Calea Victoriei, 010072 Bucharest, Romania*

*<sup>a</sup>METAV Research & Development, C.A. Rosetti, Sector 2, Bucharest, Romania*

The present work describes the influence of physical interactions among polymer constituents on the porosity of gelatin-alginate based structures. Interpenetrated polymer networks with constant gelatin loading but increasing alginate content were synthesized using a two steps cross-linking procedure. The interactions present in the biopolymers mixtures were viscometrically assessed. The morphology of the scaffolds was thereafter explained based on the dependence composition – physical forces occurring in the system before the cross-linking process. This study allows for further control of the pores size and morphology when gelatin-alginate scaffolds are needed for a specific application.

(Received March 18, 2011; accepted April 11, 2011)

*Keywords:* Porous scaffold, Physical interactions, Cross-linking, Viscometry, Gelatin-alginate

## 1. Introduction

The literature presents many attempts to produce organic scaffolds (based on synthetic or natural polymers) suitable as cells host. In this respect, many porous materials ranging from synthetic polymers such as poly(2-hydroxyethyl methacrylate) [1,2] to natural ones such as chitosan [3,4], hyaluronan [5], gelatin (Gel) [6-8] or alginate [9,10], have been studied. The material-tissue interface represents one key element in the biointegration of natural tissues into polymer matrix [11]. Starting from this idea, we decided to create porous alginate-gel structures aimed for tissue regeneration. The interest of biomaterials researchers in alginate and gel is based on one hand on their chemical nature (polysaccharide and collagenic protein) and, on the other, on their properties including the gelling capacity, the generation of 3D materials as well as the possibility to physically and chemically functionalize them. Hydrogels based on calcium alginate have been investigated and used for a wide range of biomedical applications including cell encapsulation [12-15] and delivery of bioactive species [16-21]. Their potential in stimulating calcification when combined with gel was recently explored by our group [10]. Thus, we have investigated the potential of biomimetic calcification of alginate-Gel scaffolds with porous structure and it seemed that the whole process' occurrence was related to the intensity of the interaction between the polymer chains before the cross-linking steps [10]. This is why we have decided to go back for a deeper understanding of the phenomena. During these tests we prove the very existence of strong physical interactions between the two natural polymers. The next step is to find the optimal conditions for crosslinking, so that to obtain a porous structure with suitable and controllable size and distribution of pores. In this context, we now present a

correlation between the composition, the porosity of interpenetrated polymer networks based on alginate and gel and the physical forces developed between the functional groups of these macromolecules from the early preparative stages.

## 2. Materials and methods

### 2.1 Materials

Gel B (cell culture tested) obtained by the alkaline treatment of bovine collagen was supplied from Sigma-Aldrich and used as received. Pharmaceutical grade, low viscosity sodium alginate (SA) rich in  $\alpha$ -L-guluronic residues (approx. 70% of G-block content) was purchased from Medipol SA (Lausanne, Switzerland) and used as such. Glutaraldehyde (GA) was supplied from Sigma-Aldrich as 25% solution in water. Calcium chloride dihydrate and sodium azide were supplied from Sigma-Aldrich and used as received. Bicinchoninic Acid (BCA) kit for protein determination was purchased from Sigma-Aldrich and used as such. The kit contained reagent A: BCA solution and reagent B: 4 % (w/v)  $\text{CuSO}_4 \cdot 5\text{H}_2\text{O}$  solution.

### 2.2 Scaffolds preparation

Gel was dissolved in distilled water, at 40°C, to a concentration of 20% wt; sodium azide (0.1% wt) was used to prevent bacterial growth. 4% wt SA solution was prepared through the dissolution of the polysaccharide in distilled water at room temperature, under vigorous stirring. The two solutions were mixed in different proportions, keeping gel to a concentration of 10% wt in the final polymer mixtures, while five different SA

loadings corresponding to final concentrations between 0,2% (wt) and 2% (wt), respectively, were used. The corresponding solutions were denoted A-F (see Table 1).

The generation of interpenetrating networks (IPNs) was performed through a first cross-linking with GA; GA was added to theoretically cross-link 25% of the Gel amino groups. The cross-linking agent was diluted with distilled water, in order to avoid a preferential local cross-linking. Following this reaction step, the final Gel-SA compositions contain constant amount of cross-linked Gel and increasing SA amounts. Thereafter, the mixtures were poured in Petri dishes and cooled down to 4°C. After the hydrogels have hardened, they have been removed from the Petri dishes and have been immersed in aqueous CaCl<sub>2</sub> solution (five times excess with respect to the carboxyl groups) for the cross-linking of the SA, for 24 hours. The non-reacted CaCl<sub>2</sub> has been extensively removed by water-extraction.

After cross-linking the hydrogels, cylinders with 10<sup>-2</sup> m diameter and 1.5 · 10<sup>-2</sup> m height, have been cut, washed and lyophilized for 24 hours, under vacuum (0.47-0.52 mbarr) at -50°C. For the lyophilization a Labconco (FreeZone 2.5) device was used. For simplicity, the resulted materials are denoted according to the codes of their mixtures, A-F respectively.

The success of the cross-linking was proved using the basic procedure presented in [10]. Briefly, the cross-linking of gel was verified: 1) gravimetrically through the detection of the eventually uncross-linked protein released during the CaCl<sub>2</sub> treatment of the scaffolds and 2) through the quantitative UV-VIS detection of the protein released at different time intervals using the BCA kit and a CINTRA 101 double-beam UV-VIS spectrometer, under the fixed wavelength evaluation mode. The formation of calcium alginate was confirmed gravimetrically, using the method previously described [10].

### 2.3 Falling ball viscometry

The interactions between gel and SA have been investigated through the evaluation of the dynamic viscosity of the biopolymers mixtures using a Falling Ball Viscosimeter KF10 (RheoTec Messtechnik GmbH, Otterdorf-Okrilla, Germany). Measurements have been performed between 35 and 55°C and the dynamic viscosities have been calculated using the well known equation:

$$\eta = t \cdot (\rho_1 - \rho_2) \cdot K \cdot F \quad (1)$$

where  $\eta$  represents the dynamic viscosity (mPa s),  $t$  – the travelling time of the ball (s),  $\rho_1$  – the density of the ball according to the test certificate (g/cm<sup>3</sup>),  $\rho_2$  – the density of the measuring solution (g/cm<sup>3</sup>),  $K$  – the ball constant according to the test certificate (mPas·cm<sup>3</sup>/g),  $F$  – the working angle constant.

Table 1. The composition of the Gel – SA mixtures used to prepare the scaffolds.

Mixture	Gel-SA (wt : wt)
A	100 : 2
B	100 : 4
C	100 : 8
D	100 : 10
E	100 : 12
F	100 : 20

\* as calculated from the initial preparation of 100 ml of biopolymer solutions

### 2.4 Morphology examination

Morphological information with respect to the porosity, pores' interconnection and other features has been obtained through the SEM analysis of the gold-coated freeze-dried hydrogel cylinders. The analysis has been performed using a QUANTA INSPECT F SEM device equipped with a field emission gun (FEG) with a resolution of 1.2 nm and with an X-ray energy dispersive spectrometer (EDS).

### 3. Results and discussion

All the polymer mixtures have been obtained as homogeneous, viscous solutions.

**Assessment of physical interactions.** The study of the internal interactions established between the not cross-linked polymer chains was considered necessary after the preparative step. It has been noticed an increase of the viscosity of the mixtures by comparison with the simple polymer solutions. The measurements revealed strong interactions between the components due to the functional groups such as –OH, –NH<sub>2</sub>, –COOH, which are involved in hydrogen bonds. The synergetic effect depends on the concentration of the natural polymers used as components of the solutions.

In order to be able to estimate the physical interactions which appear between the two components of the mixtures, it was necessary to study the viscometric behavior of the solutions for each biopolymer used. First we have tested a gel solution (10% wt) obtained by dilution of the initial gel solution. Fig. 1 presents the variation of dynamic viscosity within the studied range of temperature (35 – 55 °C). It may be noticed that the decrease of the viscosity values is not in a significant extent. The range of values for gel is between 9 mPa s and 18 mPa s.

Within a limited temperature range, the viscosity of a polymer solution varies generally following a relation similar to that of usual liquids, provided that polymer concentration is not too high (see Eq. (2)):

$$\eta = A \varepsilon^{\frac{K_1}{RT}} \quad (2)$$

where:  $\eta$  is the viscosity of the polymer solution (mPa s),  $A$  is a pre-exponential factor (mPa s),  $R$  is the gas constant,  $T$  is the thermodynamic temperature (K) and  $E_a$  is the activation energy (J/mol).

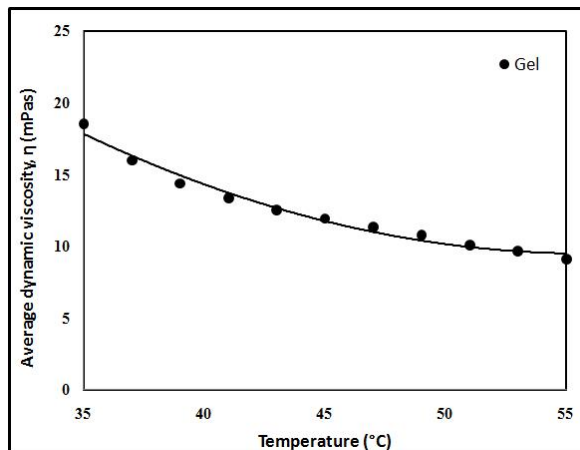


Fig. 1. The variation of the dynamic viscosities of the Gel (10%) against temperature.

After linearization of Eq. (2) it was possible to deduce the activation energy from the slope of the curve. The value for activation energy of the gel solution is 27 kJ/mol.

Concerning the SA solutions, it was experimentally established that a solution of sodium alginate cannot exceed a concentration of 4% of natural polymer. For SA solution, varying the concentration between 0,2% and 4% leads to an important increase of dynamic viscosity (see Fig. 2a). The increase presents a difference of two orders of magnitude. It can be concluded that for the concentrated solutions of SA appear an exceedingly growth of the viscosity due to a large amount of hydrogen bonds formed by dissolution of the polysaccharide in water.

By comparison with gel (10%) the less concentrated SA solutions (0.2 – 0.8 %) present smaller viscosities (see Fig. 2b).

Also all the solutions present a linear decrease of viscosity while increasing the working temperature. The effect of temperature on the activation energy in SA solutions is not important. We considered that the pre-exponential factor  $A$  is invariant with temperature, i.e. that only  $E_a$  accounts for the variation of viscosity with temperature. When the solution viscosity is considered as a function of temperature over the whole concentration domain, the experimental results are consistent with Eq. (2). It can be noticed that the activation energy remains almost constant.

The variation ranks between 18 kJ/mol and 22 kJ/mol. The major conclusion is that no additional phenomena appear except for the physical interactions between solvent and solute.

Considering the results obtained until this stage of the study, it was expected that the dynamic viscosities of the polymers mixtures to present an increment due to the physical interactions between the two solutes (the peptide contains primary amine, carboxyl, hydroxyl groups while the polysaccharide macromolecules present carboxylate and hydroxyls too).

Using the viscometric data measured for the gel-SA mixtures it could be realised a correlation between the comportment of the dynamic viscosities of simple solutions and of the mixtures. Experimental determinations confirm the theoretical expectations namely all the viscosities of gel-SA mixtures are superior to viscosities characteristic to natural polymers solutions. Fig. 3 supports this affirmation. The highest increase of the viscosity has been noticed for sample E followed by D, C, B and A. The only exception is presented by sample F which shows almost the same values for the dynamic viscosity like corresponding simple SA solution as shown in Fig. 3. This fact suggests that the polysaccharide is most likely responsible for a physical strengthening of the resulting hydrogel due to physical interactions between the peptide and the polysaccharide macromolecules, since both biopolymers are hydrosoluble and present typical functional groups that can develop hydrogen bonds; moreover, these interactions are proportional to the increase in the alginate content.

As in previous case, the activation energy remains almost constant (21 kJ/mol – 30 kJ/mol). But it can be noticed a slight increase from the simple SA solution. The increase is also due to the new physical bonds between the components of the mixtures. It was presumed [10] that this behaviour is further responsible on morphological differences of the porous scaffolds.

**Porous scaffolds.** The need for cross-linked matrices came from the application these materials were intended for, meaning scaffolds for tissue engineering (namely hard tissue engineering). Since both biopolymers used in this work are hydrosoluble and, moreover, Gel is temperature sensitive since it gels at 37 °C, without cross-linking the material would dissolve when introduced in the body. Therefore, insoluble scaffolds were synthesized through a two-step cross-linking procedure previously reported [10]. The in situ cross-linking of gel with GA led to the formation of semi-IPNs of cross-linked protein and SA. The in situ cross-linking of gel was selected as first step since due to its water solubility the protein could be lost during the  $\text{CaCl}_2$  treatment of the polymer samples. It was observed that the GA-treatment preserved the thermosensitive character of the peptide component.

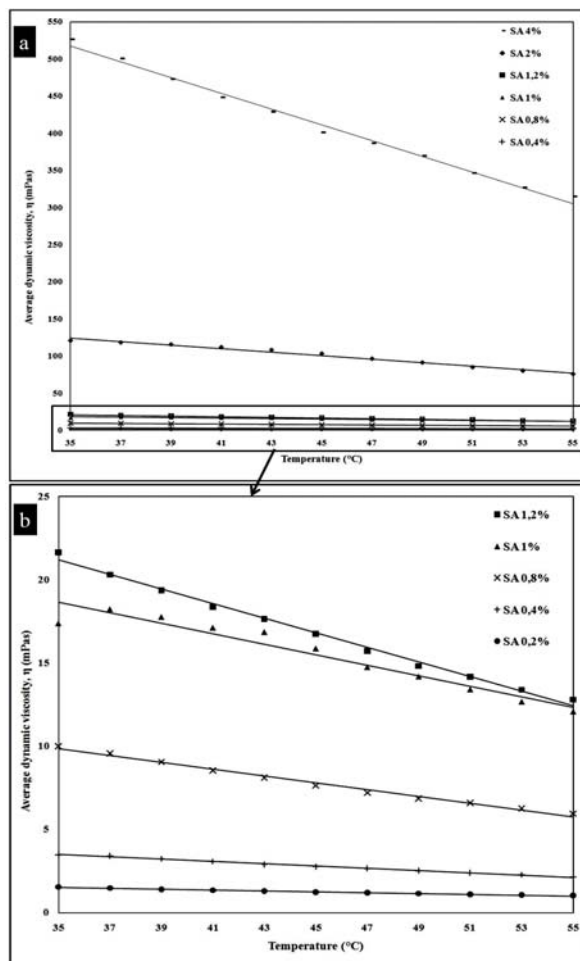


Fig. 2. The variation of the dynamic viscosities of the natural polymers solutions against temperature (a) (panel b shows a detail from panel a). The concentrations (wt/v) of the solutions are presented in the legend of the figure.

Thus, for a facile handling of the materials, the resulting mixtures were allowed to cool down to 4°C. Even if the mixtures were viscous fluids at 37°C, strong and transparent gels were obtained after decreasing the temperature. The resulted hardened semi-IPNs have been further submitted to the second step of the cross-linking.

This process involved the diffusion of CaCl<sub>2</sub> into the matrices and the high water content enhanced this process. More precisely, the semi-IPNs scaffolds were rich in water, with ratios ranging from 88 to 89 % v/v (due to the preparation of the synthesis solutions) (see Table 1). The result of the second cross-linking process consisted in gel – calcium alginate IPNs which have been further freeze-dried to generate porous structures.

The screening of the cross-linking efficiency proved the success of the hydrogels synthesis under the form of IPNs.

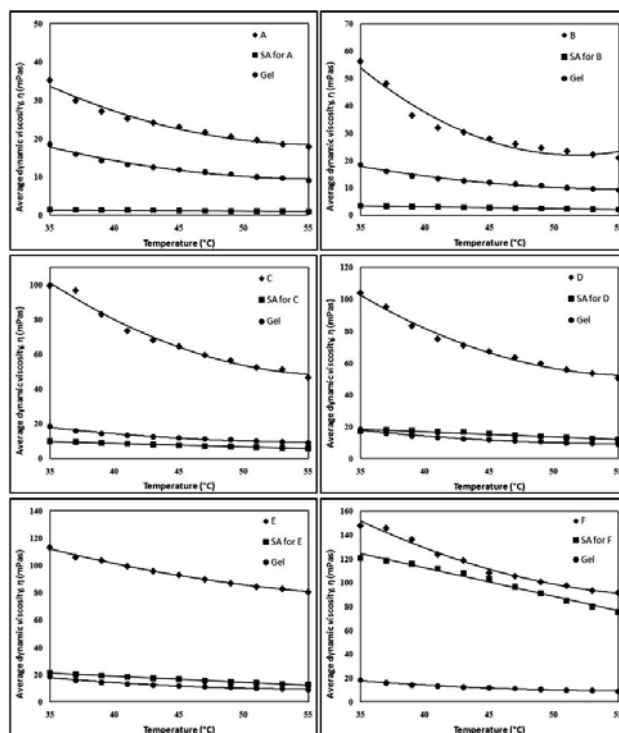


Fig. 3. The variation of dynamic viscosities with temperature for Gel-SA mixtures: A – F against the corresponding simple SA and Gel solutions.

**SEM assessment** allowed the detailed analysis of the samples morphology.

All the hydrogels presented interconnected porosity, with pores presenting certain morphological dispersity.

The pore size was measured and average values were calculated for each sample. As it may be seen from Table 2, when the initial ratio between gel and calcium alginate decreases, the final products (after the treatment previously described) show smaller size of pores; starting with maximum 450-600 μm (in sample A) the diameters of the pores decrease up to 130-150 μm (in sample E).

We should take into account that increasing the amount of CA, more and more physical contacts are formed; this feature leads to a tighter package of chains having as a result the increase of pores size.

As may be seen from Fig. 4, not only that the total size of the pores diminishes, but also the pore distribution becomes narrower. Even if we cannot express this distribution in a quantitative way, Fig. 4 illustrates the above mentioned fact.

These phenomena are in good agreement with the data proving the strong physical interactions between the two natural polymers that have been put into evidence by viscometric measurements.

The morphological examination continued with the assessment of the external surface of the porous blocks. All the samples present a continuous coating, showing the pores as packed along the longitudinal axis (Fig. 5). The

external layer does not present open pores, but exclusively closed ones.

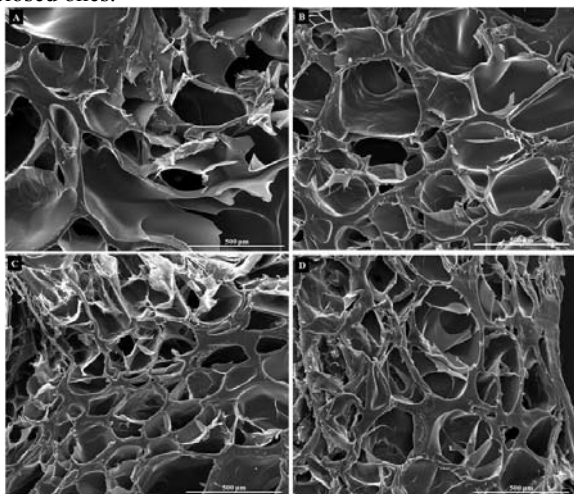


Fig. 4. SEM image displaying the porosity and the interconnectivity of the pores (as obtained from the analysis of cross-sections) of sample A-D.

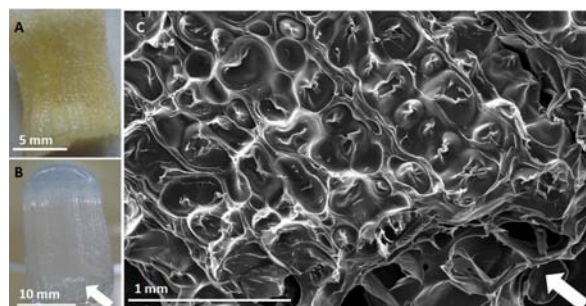


Fig. 5. Porous hydrogels (PA) freeze dried (A), rehydrated (B), SEM image taken from its external surface (C); multiple spherical pores seem longitudinally packed, coated by a polymer continuous layer; the cross-section (indicated by the white arrow) shows open pores, with diameters of about 450  $\mu\text{m}$ .

Nevertheless, the cross-section proves the existence of the open pores inside the materials. The SEM image described in panel C from Fig. 5 is in good agreement with the morphology of the scaffolds displayed in panels A and B.

Table 2. Identifiers for the porous samples, their correspondence with the preparative solutions and the average dimensions of the pores.

Porous hydrogel produced from mixtures (see Table 1)	Average size of the pores in the porous scaffold ( $\mu\text{m}$ )
A	450-600
B	500-350
C	250-330
D	170-200
E	130-150
F*	-

\* not characterized; the cross-linked material was non-homogeneous

Quite interesting, the walls of the pores present smooth surfaces, whose thick increases with CA content, while the external layer of the samples contain fibrillar longitudinal structures separating the packed pores of the constructs (Fig. 6).

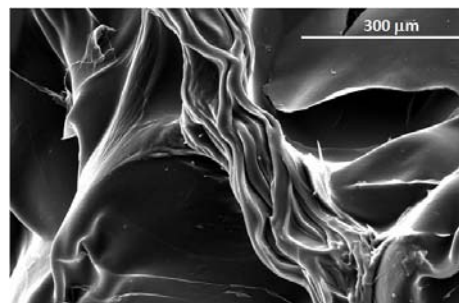


Fig. 6. Longitudinal polymeric rod-like separation fibrillar structures appear between the packed pores, while the internal walls of the pores are smooth.

#### 4. Conclusions

The present paper correlates the morphology of the scaffolds (in terms of porosity) with the intensity of the physical interactions expressed between the constitutive biopolymers.

Viscometric measurements on solutions of natural polymers, as well as on the mixtures of these ones proved an increased viscosity with increasing the alginate content. The tests have shown a synergetic behaviour, this being an indirect proof for strong physical interactions are developed between the biopolymers chains. To the best of our knowledge, there are not studies concerning the viscometric compartment of natural polymers mixtures. We have found a technique capable to produce organic networks with a pre – designed porosity.

#### Acknowledgments

The financial support from the European Social Fund through POSDRU/89/1.5/S/54785 project "Postdoctoral Program for Advanced Research in the field of nanomaterials" is acknowledged.

#### References

- [1] X. Lou, S. Munro, S. Wang, *Biomaterials* **25**, 5071 (2004).
- [2] I. C. Stancu, P. Layrolle, H. Libouban, R. Filmon, G. Legeay, C. Cincu, M. F. Basle, D. Chappard, *J. Optoelectron. Adv. Mater.* **7**, 2125 (2007).
- [3] D. M. Garcia Cruz, D. F. Coutinho, J. F. Mano, J. L. Gomez Ribelles, M. Salmeron Sanchez, *Polymer* **50**, 2058 (2009).
- [4] A. R. C. Duarte, J. F. Mano, R. L. Reis *J. Supercrit. Fluids*, **54**, 282 (2010).

- [5] D. B. Pike, S. Cai, K. R. Pomraning, M. A. Firpo, R. J. Fisher, X. Z. Shu, G. D. Prestwich, R. A. Peattie, *Biomaterials* **27**, 5242 (2006).
- [6] I. C. Stancu, *React. Funct. Polym.* **70**, 314 (2010).
- [7] P. Dubruel, R. Unger, S. Van Vlierberghe, V. Cnudde, P. J. S. Jacobs, E. Schacht, C. J. Kirkpatrick, *Biomacromol.* **8**, 338 (2007).
- [8] A. Van Den Bulcke, B. Bogdanov, N. De Rooze, E. Schacht, M. Cornelissen, H. Berghmans, *Biomacromol.* **1**, 31 (2000).
- [9] S. Ch. Chen, Y. Ch. Wu, F. L. Mi, Y. H. Lin, L. Ch. Yu, H. W. Sung, *J. Control. Rel.* **96**, 285 (2004).
- [10] I. C. Stancu, D. M. Dragusin, E. Vasile, R. Trusca, I. Antoniac, D. S. Vasilescu, *J Mater Sci: Mater Med*, DOI 10.1007/s10856-011-4233-7 (2010).
- [11] D. A. Puleo, A. Nanci, *Biomaterials*, **20**, 2311 (1999).
- [12] S. Gerech-Nir, S. Cohen, A. Ziskind, J. Itskovitz-Eldor, *Biotechnol. Bioeng.*, **88**, 313 (2004).
- [13] S. C. N. Chang, J. A. Rowley, G. Tobias, N. G. Genes, A. K. Roy, D. J. Mooney, Ch. A. Vacanti, L. J. Bonassar, *J. Biomed. Mater. Res.* **55**, 503 (2001).
- [14] E. Fragonas, M. Valente, M. Pozzi-Mucelli, R. Toffanin, R. Rizzo, F. Silvestri, F. Vittur, *Biomaterials* **21**, 795 (2000).
- [15] K. Kataoka, Y. Suzuki, M. Kitada, K. Ohnishi, K. Suzuki, M. Tanihara, Ch. Ide, K. Endo, Y. Nishimura, *J. Biomed. Mater. Res.* **54**, 373 (2001).
- [16] T. Sone, E. Nagamori, T. Ikeuchi, A. Mizukami, Y. Takakura, S. Kajiyama, E.-i. Fukusaki, S. Harashima, A. Kobayashi, K. Fukui, *J. Biosci. Bioeng.* **94**, 87 (2002).
- [17] T. Higashi, E. Nagamori, T. Sone, S. Matsunaga, K. Fukui, *J. Biosci. Bioeng.* **97**, 191 (2004).
- [18] M. Sivakumar, K. Panduranga Rao, *J. Biomed. Mater. Res. A* **65**, 222 (2003).
- [19] A. Perets, Y. Baruch, F. Weisbuch, G. Shoshany, G. Neufeld, S. Cohen, *J. Biomed. Mater. Res. A* **65**, 489 (2003).
- [20] P. Eiselt, J. Yeh, R. K. Latvala, L. D. Shea, D. J. Mooney, *Biomaterials* **21**, 1921 (2000).
- [21] B. Amsden, N. Turner, *Biotechnol. Bioeng.* **65**, 605 (1999).

---

\*Corresponding author: dsvasilescu@gmail.com